Effect of Interfacial Viscosities upon Displacement in Sinusoidal Capillaries

This quantitative analysis shows the relative effects of interfacial tension, interfacial viscosities, and wetting during displacement in a capillary whose radius is a sinusoidal function of axial position. The effect of the interfacial viscosities is to increase the resistance to displacement regardless of the wetting condition. The results are consistent with a previous qualitative analysis and with a previous quantitative analysis for displacement in capillaries whose radii are independent of axial position.

In screening surfactant systems for potential use in tertiary oil recovery, it is recommended that the interfacial tension be minimized first, since it determines whether oil displacement will occur, and that the interfacial viscosities be minimized second, since they influence the rate of oil displacement.

R. M. Giordano, J. C. Slattery
Department of Chemical Engineering
Northwestern University
Evanston, IL 60201

Introduction

Conventional production of light crudes usually concludes with a partial displacement of the oil remaining in the reservoir by either water or brine. For carefully selected, well-designed, good-performing operations, at the end of conventional petroleum production there remains trapped 50–70% of the oil originally in place (Geffen, 1973).

Residual oil is trapped in the form of blobs, each of which occupies possibly a large set of neighboring pores. Once such a blob has been isolated, it may or may not continue to be driven forward by the existing pressure gradient (Slattery, 1974; Oh and Slattery, 1979). If one of its many phase interfaces does advance, it will do so in an episodic fashion: it will slowly creep forward until an instability develops somewhere in the system, it will jump ahead a short distance, and it will begin another period of creeping motion. Since these Haines (1930) jumps take place very rapidly (Heller, 1968), the displacement of residual oil appears to be controlled by the period of slow advancement between jumps.

Slattery (1974, 1979) developed a qualitative analysis for these periods of creeping motion. He was able to draw a number of conclusions, one of which is that, when the interfacial tension is less than the critical value required for displacement and the interfacial viscosities are large, equal percentage reductions of the interfacial tension and the interfacial viscosities are equally important (Giordano and Slattery, 1983a). (When the interfacial viscosities are small, it is more important to reduce the interfacial tension.) This conclusion has been fully supported both by a quantitative analysis (Giordano and Slattery, 1983a) and by an experimental study (Stoodt and Slattery, 1984) of displacement in capillaries whose radii are independent of axial position.

The pores in an oil-bearing rock are not that simple, and an exact solution to the equations of motion for such a porous medium is impractical. In order to simulate displacements under these conditions, we recommend speaking in terms of local volume averages at each point in the region occupied by the porous media and the fluids it contains (Slattery, 1981). As a result of averaging, information is lost and the local volume-averaged equations of motion are expressed in terms of several integrals or functions: the permeability, the relative permeability of the wetting phase, the relative permeability of the nonwetting phase, the capillary pressure. The information lost as a result of local volume averaging must be replaced by supplying explicit forms for these functions. The usual approach is to construct empirical data correlations. As one attempts to account for additional physical phenomena, this becomes more difficult. An alternative approach is to construct a structural model or idealized model for the local flow field within the averaging volume associated with each point in the porous medium.

Network models that focus on the mechanism of oil entrapment and the distribution of residual oil generally neglect the dynamics of flowing oil droplets (ganglia). These models apply

The current address of R. M. Giordano is ARCO Oil and Gas Co., Plano, TX 75075.

to quasi-static processes, in which most of the interfaces are static most of the time; the key mechanisms considered are the choke-off and jumps of interfaces (Mohanty et al., 1980; Lin and Slattery, 1982). Frequently, one is more interested in the rate of displacement, when many interfaces are moving at once. This can be investigated with models that explicitly include the dynamics of oil displacement (Dias and Payatakes, 1986a,b; Aleman et al., 1986). These dynamic models require an expression for the rate of displacement in an idealized pore as a function of the pressure drop and various physical parameters such as the interfacial tension, the contact angle, and the interfacial viscosities (Washburn, 1921; Giordano and Slattery, 1983a).

Static analyses (Oh and Slattery, 1979; Giordano and Slattery, 1983b) suggest that pore geometry plays an important role in displacement and that it should not be ignored in devising structural models to be used in the context of local volume averaging. In this paper, we extend our previous analysis for displacement (Giordano and Slattery, 1983a) to sinusoidal capillaries. In particular, we account here for the influence of the interfacial viscosities as the interface expands and contracts in moving through a sinusoidal capillary.

Statement of Problem

Figure 1 shows phase 1 displacing phase 2 in a capillary whose radius r_w^* is a sinusoidal function of axial position z^* measured with respect to a frame of reference in which the capillary wall is stationary,

$$r_w \equiv \frac{r_w^*}{r_n^*} = 1 + \frac{B}{2}\left[1 - \cos\left(\frac{2\pi z}{\ell}\right)\right] \tag{1}$$

in which

$$z \equiv \frac{z^*}{r_n^*} \quad \ell \equiv \frac{\ell^*}{r_n^*} \quad B \equiv \frac{B^*}{r_n^*} \tag{2}$$

and r_n^* is the neck or throat radius. Fluid moves through the pore at an average flowrate Q_{avg}^*, which causes the common line C, formed by the intersection of the fluid-fluid interface Σ with the wall, to be displaced. The contact angle α is measured through phase 1. The axial positions of the imaginary surfaces $S^{(1)}$ and $S^{(2)}$ are fixed with respect to the capillary wall.

Our objective is to estimate Q_{avg}^* for a given pressure drop between $S^{(1)}$ and $S^{(2)}$.

With three minor exceptions, the assumptions of Giordano and Slattery (1983a) apply, so long as the characteristic length is taken to be r_n^* and the characteristic speed $Q_{avg}^*/(\pi r_n^{*2})$. The exceptions are to their assumptions j, k, and l.

j. We have neglected the work done by viscous forces on the surfaces $S^{(1)}$ and $S^{(2)}$. This would be exact if the radius of the capillary were independent of axial position.

k. Consider the system composed of those portions of phases 1 and 2 in the tube between $S^{(1)}$ and $S^{(2)}$. In forming the integral mechanical energy balance for this system, we have estimated the rate of viscous dissipation of mechanical energy within the bulk phases, neglecting the influence of Σ and neglecting any work done by viscous forces at the entrance and exit cross sections for each phase (see assumption j).

l. In this integral mechanical energy balance, we have neglected the work done by the viscous surface stress at the common line, assuming that the contact angle measured at the common line is unaffected by small perturbations of the capillary number N_{ca} from zero. This would be exact if the contact angle measured within the immediate neighborhood of the common line were 0°. The work by Wayner (1980) and Teletzke et al. (1982) suggests that the microscopic contact angle is 0°, even though the macroscopically observed contact angle may not be zero.

Interfacial Velocity Distribution

Our initial objective is to determine the interfacial velocity distribution for the displacement shown in Figure 1. We seek a perturbation solution that is correct to the zeroth order in N_{ca}, $(N_{\kappa+\epsilon})^{-1}$, $N_{Re}^{(1)}$, $N_{Re}^{(2)}$, N_{Bo}, and the slip ratio (Giordano and Slattery, 1983a).

In our analysis, all variables marked * are dimensional. It will be convenient to introduce as dimensionless variables

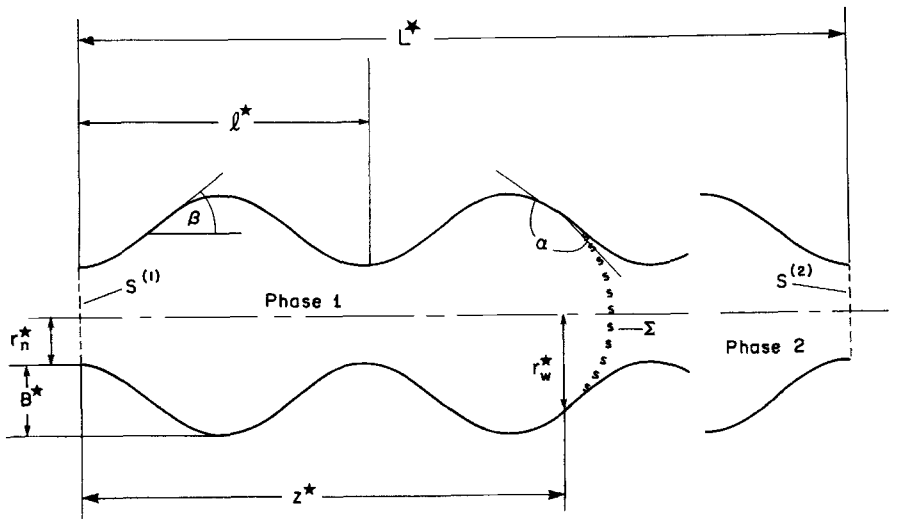

Figure 1. Phase 1 displacing phase 2 in a sinusoidal capillary.

$$v^{(J)} \equiv \frac{\pi r_n^{*2} v^{(J)*}}{Q^*_{avg}} \qquad v^{(\sigma)} \equiv \frac{\pi r_n^{*2} v^{(\sigma)*}}{Q^*_{avg}}$$

$$S^{(J)} \equiv \frac{\pi r_n^{*3} S^{(J)*}}{\mu^{(J)*} Q^*_{avg}} \qquad S^{(\sigma)} \equiv \frac{\pi r_n^{*3} S^{(\sigma)*}}{(\kappa^* + \epsilon^*) Q^*_{avg}}$$

$$p^{(J)} \equiv r_n^* p^{(J)*}/\gamma^* \qquad \bar{r} \equiv \bar{r}^*/r_n^*$$

$$H \equiv r_n^* H^* \tag{3}$$

in which $(\bar{r}^*, \bar{\theta}, \bar{\phi})$ are the spherical coordinates in a frame of reference that is fixed with respect to the center of curvature of the interface, and H^* is the mean curvature of the interface. A frame of reference that is fixed with respect to the center of curvature of the interface is found in the next section to be convenient in estimating the rate of viscous dissipation of energy within the interface.

Viewed in this frame of reference, the solution takes the same form as that developed by Giordano and Slattery (1983a) for displacement in a capillary whose radius is independent of axial position. The interface is a spherical segment and the interfacial velocity has only one nonzero component

$$\bar{v}_{\bar{\theta}}^{(\sigma)} = \bar{v}_c \frac{P_\nu^{-1}(\cos \bar{\theta})}{P_\nu^{-1}[\sin (\alpha + \beta)]} \tag{4}$$

in which β is defined in terms of the slope of the capillary wall

$$\tan \beta \equiv \frac{dr_w}{dz} = \frac{\pi B}{\ell} \sin\left(\frac{2\pi z}{\ell}\right) \tag{5}$$

for $-(\pi/2) \le \beta \le (\pi/2)$ and ν satisfies

$$\nu(\nu + 1) = \frac{2\epsilon^*}{\kappa^* + \epsilon^*} \tag{6}$$

In reaching this result, we have specified

$$\text{at } \bar{\theta} = \left| \alpha + \beta - \frac{\pi}{2} \right| : \bar{v}_{\bar{\theta}}^{(\sigma)} = \bar{v}_c \tag{7}$$

leaving $\bar{v}_c$ for the moment unspecified.

Following the argument of Giordano and Slattery (1983a), we conclude that in a frame of reference fixed with respect to the common line,

$$\text{at common line: } \hat{v}^{(\sigma)} \cdot \mathbf{g}_{\bar{\theta}} = A \hat{v}_w \tag{8}$$

in which $\bar{v}_w$ is the magnitude of the dimensionless velocity of the wall,

$$\begin{aligned} A \equiv -\{&N_\mu[\alpha \cos \alpha - \sin \alpha][\sin^2 \alpha - (\alpha - \pi)^2] \\ &+ [(\alpha - \pi) \cos \alpha - \sin \alpha][\alpha^2 - \sin^2 \alpha]\} \\ &\cdot \{N_\mu[\sin \alpha \cos \alpha - \alpha][(\alpha - \pi)^2 - \sin^2 \alpha] \\ &+ [\alpha - \pi - \sin \alpha \cos \alpha][\alpha^2 - \sin^2 \alpha]\}^{-1} \end{aligned} \tag{9}$$

is shown in Figure 2, and

$$N_\mu \equiv \mu^{(1)*}/\mu^{(2)*} \tag{10}$$

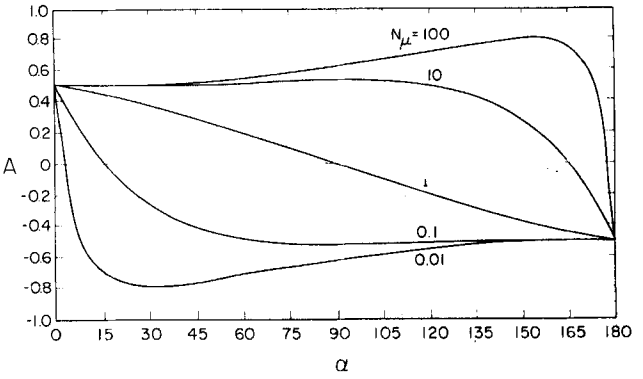

Figure 2. Function *A* defined by Eq. 10.

In appendix A, we argue that

$$\bar{v}_{\bar{\theta}}^{(\sigma)} = \hat{v}^{(\sigma)} \cdot \mathbf{g}_{\bar{\theta}} - \frac{r_{wc}}{\cos (\alpha + \beta)} \frac{d\beta}{dt} \tag{11}$$

with the understanding that r_{wc} is the dimensionless radius of the capillary at the common line,

$$t \equiv \frac{Q^*_{avg} t^*}{\pi r_n^{*3}} \tag{12}$$

is dimensionless time and the time derivative follows the motion of the common line. Differentiating Eq. 5, we find

$$\frac{d\beta}{dt} = \frac{2\pi^2 B}{\ell^2} v_\Sigma \cos^2 \beta \cos\left(\frac{2\pi z_c}{\ell}\right) \tag{13}$$

Here z_c is the dimensionless axial position of the common line measured with respect to a frame of reference in which the capillary is stationary and

$$v_\Sigma \equiv \frac{dz_c}{dt} \tag{14}$$

In appendix B, we find

$$\text{at common line: } \hat{v}_w \equiv |\hat{v}_w| = v_\Sigma \left\{1 + \left[\frac{\pi B}{\ell} \sin\left(\frac{2\pi z_c}{\ell}\right)\right]^2\right\}^{1/2} \tag{15}$$

From Eqs. 7, 8, 11, 13, and 15, we conclude

$$\begin{aligned} K_1 \equiv \bar{v}_c/v_\Sigma = A &\left\{1 + \left[\frac{\pi B}{\ell} \sin\left(\frac{2\pi z_c}{\ell}\right)\right]^2\right\}^{1/2} \\ &- \frac{2\pi^2 r_{wc} B \cos^2 \beta}{\ell^2 \cos (\alpha + \beta)} \cos\left(\frac{2\pi z_c}{\ell}\right) \end{aligned} \tag{16}$$

In a frame of reference that is fixed with respect to the center of curvature of the interface, the normal component of interfacial velocity is

$$\bar{v}_{(\bar{\xi})}^{(\sigma)} = \bar{v}^{(\sigma)} \cdot \mathbf{g}_{\bar{r}} = \frac{d}{dt}\left(\frac{r_w}{\sin \bar{\theta}_c}\right) \tag{17}$$

in which we have noted that $\bar{\theta} = \bar{\theta}_c$ at the common line. Using Eqs. 1 and 13, we find

$$K_2 \equiv \bar{v}^{(\sigma)}_{(\xi)}/v_\Sigma = \frac{\pi B}{\ell}\frac{1}{|\cos(\alpha+\beta)|}\left[\sin\left(\frac{2\pi z_c}{\ell}\right) + \frac{2\pi r_w}{\ell}\frac{\tan(\alpha+\beta)}{\sec^2\beta}\cos\left(\frac{2\pi z_c}{\ell}\right)\right] \tag{18}$$

Integral Mechanical Energy Balance

Our objective is to estimate the volume rate of flow through the capillary shown in Figure 1 for a given pressure drop between $S^{(1)}$ and $S^{(2)}$. In what follows, our frame of reference will be fixed with respect to the capillary wall.

We have previously shown that an integral mechanical energy balance for the system $R_{(sys)}$ consisting of those portions of phases 1 and 2 in the capillary between $S^{(1)}$ and $S^{(2)}$ requires (Giordano and Slattery, 1983a)

$$\int_{S_{(sys)}}(-p^*\boldsymbol{v}^*\cdot\boldsymbol{n}+\boldsymbol{v}^*\cdot\boldsymbol{S}^*\cdot\boldsymbol{n})\,dA^* = \int_{R_{(sys)}}\mathrm{tr}(\boldsymbol{S}^*\cdot\nabla\boldsymbol{v}^*)\,dV^* + \int_\Sigma\{-2H^*\gamma\boldsymbol{v}^{(\sigma)*}\cdot\boldsymbol{\xi} + \mathrm{tr}(\boldsymbol{S}^{(\sigma)*}\cdot\boldsymbol{D}^{(\sigma)*})\}\,dA^* - \int_C \boldsymbol{v}^{(\sigma)*}\cdot\boldsymbol{S}^{(\sigma)*}\cdot\boldsymbol{\mu}\,ds^* \tag{19}$$

In view of assumption j, the integral on the lefthand side of Eq. 19 takes the form

$$\int_{S_{(sys)}}(-p^*\boldsymbol{v}^*\cdot\boldsymbol{n}+\boldsymbol{v}^*\cdot\boldsymbol{S}^*\cdot\boldsymbol{n})\,dA^* = Q^*\Delta p^* \tag{20}$$

Considering assumption k, we can write a mechanical energy balance for each individual phase to conclude

$$\int_{R_{(sys)}}\mathrm{tr}(\boldsymbol{S}^*\cdot\nabla\boldsymbol{v}^*)\,dV^* = \frac{Q^{*2}C}{\pi\ell^* r_n^{*3}}[\mu^{(1)*}z_c^* + \mu^{(2)*}(L^*-z_c^*)] \tag{21}$$

Here we have employed the result of Neira and Payatakes (1979; see also Tilton and Payatakes, 1984) for the pressure drop over one unit of a sinusoidal pore

$$\Delta p^{(j)*} = \frac{C\mu^{(j)*}Q^*}{\pi r_n^{*3}} \tag{22}$$

where C is given by their Figure 1. [Note that their $-\Delta P_1^*$ is our C, their r_1^* is our ℓ^{-1}, and their r_2^* is our $(1+B)/\ell$.]

In writing Eq. 21 we have neglected the effects of the interface upon bulk viscous dissipation. This assumption is typical of equations like those of Washburn (1921), whose validity has been verified in both uniform (Rose and Heins, 1962) and converging-diverging (Legait et al., 1983) capillaries. Since the bulk flow is affected by the interface in a region approximately one tube radius on either side of the interface (Goldsmith and Mason, 1963), assumption k can be expected to fail in the limit of closely spaced, small segments.

In Eq. 21, we have made the simplistic assumption that bulk viscous dissipation is proportional to the axial distance between the common lines defining the leading and trailing interfaces. A more detailed computation such as that given by Dias and Payatakes (1986a) does not appear to be justified here, since the contribution of the bulk viscous dissipation is small for our analysis in which $N_{\epsilon+\epsilon} \gg 1$ (see Eqs. 30 and 34).

By assumption ℓ, we will say

$$\int_C \boldsymbol{v}^{(\sigma)*}\cdot\boldsymbol{S}^{(\sigma)*}\cdot\boldsymbol{\mu}\,ds^* = 0 \tag{23}$$

With the approximation that the configuration of the interface can be represented as a spherical segment (assumption n of Giordano and Slattery, 1983a)

$$\int_\Sigma 2H^*\gamma^*\boldsymbol{v}^{(\sigma)*}\cdot\boldsymbol{\xi}\,dA^* = \frac{2Q^*\gamma^*\cos(\alpha+\beta)}{r_{wc}^*} \tag{24}$$

The rate of viscous dissipation of energy within the interface is frame-indifferent. We will find it more convenient to estimate it in a frame of reference that is fixed with respect to the center of curvature of the interface. Recognizing assumption m of Giordano and Slattery, we can employ Green's transformation for a surface (McConnell, 1957) to write

$$\int_\Sigma \mathrm{tr}[\boldsymbol{S}^{(\sigma)*}\cdot\boldsymbol{D}^{(\sigma)*}]\,dA^* = \int_\Sigma \mathrm{tr}[\bar{\boldsymbol{S}}^{(\sigma)*}\cdot\bar{\boldsymbol{D}}^{(\sigma)*}]\,dA^* = -\int_{\Sigma_0}\bar{\boldsymbol{v}}^{(\sigma)*}\cdot\mathrm{div}_{(\sigma)}\bar{\boldsymbol{S}}^{(\sigma)*}\,dA^* + \int_{C_0}\bar{\boldsymbol{v}}^{(\sigma)*}\cdot\bar{\boldsymbol{S}}^{(\sigma)*}\cdot\bar{\boldsymbol{\mu}}\,dS^* \tag{25}$$

in which we have found it convenient to denote Σ_0 as that portion of the interface outside the immediate neighborhood of the common line and C_0 as the closed curve (circle) bounding Σ_0. Remembering that in this frame of reference the radius of curvature of the interface changes with time, the first term on the righthand side of Eq. 25 takes the form

$$\int_{\Sigma_0}\bar{\boldsymbol{v}}^{(\sigma)*}\cdot\mathrm{div}_{(\sigma)}\bar{\boldsymbol{S}}^{(\sigma)*}\,dA^* = 2\pi(\kappa^*+\epsilon^*)(v_\Sigma^*)^2\cdot\left((K_1)^2\left\{(1-\nu)\frac{P_{\nu-1}^{-1}[\sin(\alpha+\beta)]}{P_\nu^{-1}[\sin(\alpha+\beta)]} + (1-\nu^2)\sin(\alpha+\beta)\right\} + 2\left(\frac{\kappa^*}{\kappa^*+\epsilon^*}\right)K_1K_2|\cos(\alpha+\beta)|\right) \tag{26}$$

where K_1 and K_2 are given by Eqs. 16 and 18. In contrast with Eq. 23, the second term on the righthand side of Eq. 25 has the value

$$\int_{C_0}\bar{\boldsymbol{v}}^{(\sigma)*}\cdot\bar{\boldsymbol{S}}^{(\sigma)*}\cdot\bar{\boldsymbol{\mu}}\,ds^* = 2\pi\nu^*(v_\Sigma^*)^2[K_1K_2|\cos(\alpha+\beta)| - (K_1)^2\sin(\alpha+\beta) + 2(K_1)^2] \tag{27}$$

With Eqs. 26 and 27, Eq. 25 may be more conveniently expressed as

$$\int_\Sigma \mathrm{tr}(\boldsymbol{S}^{(\sigma)*}\cdot\boldsymbol{D}^{(\sigma)*})\,dA = 2\pi(\kappa^*+\epsilon^*)(v_\Sigma^*)^2E \tag{28}$$

in which we have defined

$$E \equiv (K_1)^2 \left\{ (1-\nu) \frac{P_{\nu-1}^{-1}[\sin(\alpha+\beta)]}{P_\nu^{-1}[\sin(\alpha+\beta)]} + (1-\nu^2)\sin(\alpha+\beta) \right\} + 4\left(\frac{\kappa^*}{\kappa^*+\epsilon^*}\right) K_2 \{K_1 |\cos(\alpha+\beta)| + K_2[1-\sin(\alpha+\beta)]\} \quad (29)$$

Finally, with the help of Eqs. 20, 21, 23, 24, and 28, we can arrange the integral mechanical energy balance Eq. 19 in the more convenient form

$$\frac{Q^*\mu^{(2)*}}{|\Delta p^*|\pi r_n^{*3}} = \left[\frac{\Delta p^*}{|\Delta p^*|} + 2N_\gamma \frac{\cos(\alpha+\beta)}{r_{wc}}\right] \cdot \left\{ C\left[\frac{z_c}{\ell}(N_\mu - 1) + \frac{L^*}{\ell^*}\right] + 2N_{\kappa+\epsilon} r_{wc}^{-4} E \right\}^{-1} \quad (30)$$

where

$$N_\gamma \equiv \frac{\gamma^*}{|\Delta p^*| r_n^*} \quad (31)$$

Usually we will be more concerned with the average volume rate of flow Q^*_{avg}

$$Q^*_{avg} = V^*_{pore} \left(\int_{\ell^*}^{2\ell^*} \frac{dz^*}{v_\Sigma^*} \right)^{-1} \quad (32)$$

Here V^*_{pore} is the volume of a unit pore

$$V^*_{pore} = \pi (r_n^*)^3 \int_0^{\ell} (r_w)^2 \, dz \quad (33)$$

in which r_w is described by Eq. 1.

For the displacement of a segment of phase 2 through a capillary filled with phase 1 shown in Figure 3, we can immediately say by analogy with Eq. 30 that

$$\frac{Q^*\mu^{(2)*}}{|\Delta p^*|\pi r_n^{*3}} = \left\{ \frac{\Delta p^*}{|\Delta p^*|} - 2N_\gamma \left[\frac{\cos(\alpha_R - \beta_R)}{r_{wcR}} - \frac{\cos(\alpha_L + \beta_L)}{r_{wcL}} \right] \right\} \cdot \left\{ C\left[\frac{1}{\ell}(z_{cL} - z_{cR})(N_\mu - 1) + \frac{L^*}{\ell^*} N_\mu\right] + 2N_{\kappa+\epsilon}(r_{wcL})^{-4} \left[E_L + \left(\frac{r_{wcL}}{r_{wcR}}\right)^4 E_R \right] \right\}^{-1} \quad (34)$$

where

$$E_L \equiv E(\alpha_L, N_\mu, z_{cL})$$
$$E_R \equiv E(\pi - \alpha_R, N_\mu^{-1}, z_{cR}) \quad (35)$$

The subscript L refers to the left interface in Figure 3 and the subscript R refers to the right interface.

Discussion

The void volume in a permeable rock, such as that in which oil is found, may be thought of as many intersecting pores of varying diameters. Consider two neighboring pore networks having different mean radii that offer parallel paths for displacement. Oil will be trapped in that pore network through which the oil is displaced more slowly. The rate at which this residual oil can be mobilized determines the efficiency of a tertiary oil flood.

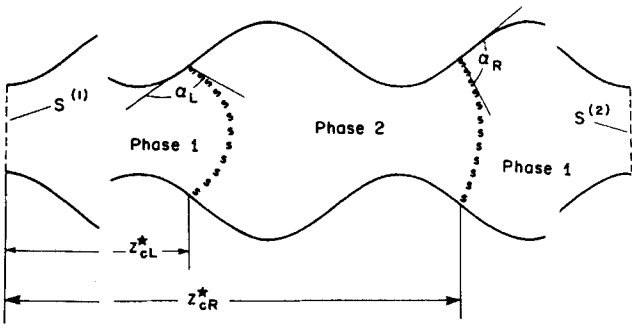

Figure 3. Segment of phase 2 being displaced through a sinusoidal capillary initially filled with phase 1.

We shall approximate this rate by using the system shown in Figure 3 as an idealization of a pore in which residual oil is trapped. Equation 34 shows that for a given pressure drop there exists a critical value of N_γ above which there can be no displacement of oil. Oh and Slattery (1979) show how this critical value changes with pore geometry. Giordano and Slattery (1983b) have investigated the effects of contact angle hysteresis on N_γ.

Because the rate of viscous dissipation of energy must be positive both in the bulk phases and in the interface, Eqs. 21 and 28 show that the denominators of Eqs. 30 and 34 are always positive regardless of the value of the contact angle and the configuration of the pore wall. Equations 30 and 34 predict that, when the interfacial tension is below the critical value required for displacement, the effect of the interfacial viscosities is to decrease the rate of displacement.

For tertiary oil recovery systems, $N_{\kappa+\epsilon} \gg 1$. The limited data currently available indicate that the crude oil-brine interfacial shear viscosity prior to the addition of a surfactant can be large, ~1 mN · s/m (Jones et al., 1978), which may be attributable to a mixture of natural surfactants in the oil (Strassner, 1968). It may also be relatively small, ~0.01 mN · s/m (Wasan et al., 1978). The measurements of Stoodt and Slattery (1984) suggest that the interfacial dilatational viscosity may be two orders of magnitude larger than the interfacial shear viscosity. If we assume that $r_n^* = 10$ μm (Batra and Dullien, 1973), that $\mu^{(2)*} = 1$ mPa · s, and that $(\kappa^* + \epsilon^*) = 0.01$ mN · s/m (a conservative estimate), we conclude that $N_{\kappa+\epsilon} \sim 10^3$.

To demonstrate the relative effects of the interfacial tension and the interfacial viscosities, consider a system for which $r_n^* = 10$ μm (Batra and Dullien, 1973) and $L^*/r_n^* = 24$. Consistent with Oh and Slattery (1979), we choose $B = 1.5$, $\ell = 6$, $\alpha_L = 140°$, $\alpha_R = 38°$, and $V_{drop} = V^*_{drop}/r_n^{*3} = 80$, where V^*_{drop} is the volume of the segment of phase 2. [These contact angles correspond to an intrinsic contact angle $\alpha_{int} = 89°$, if we assume Morrow's (1975) class III contact angle hysteresis. This is a case of intermediate wettability.] We identify phase 1 as brine, phase 2 as oil, and $N_\mu = 0.1$. We will conservatively estimate $\kappa^*/\epsilon^* = 1$, although the data of Stoodt and Slattery (1984) suggest that the surface dilatational viscosity may be two orders of magnitude larger than the surface shear viscosity.

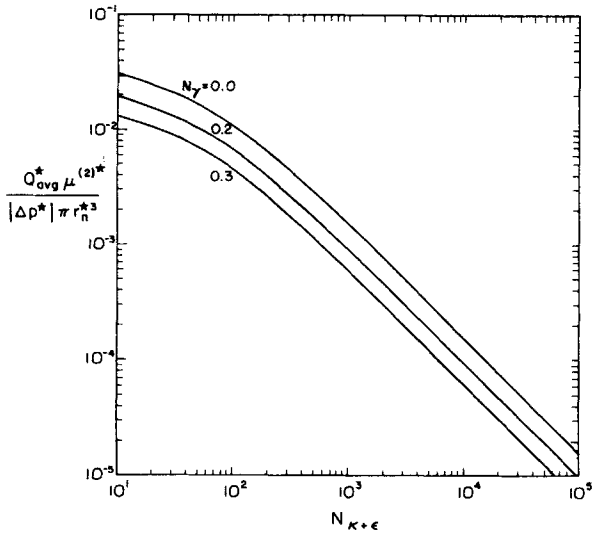

Figure 4. Average flow rate for displacement of a segment of phase 2 in a capillary initially filled with phase 1 as a function of $N_{\kappa+\epsilon}$

$N_\mu = 0.1$; $\alpha_L = 140°$; $\alpha_R = 38°$; $V_{drop} = 80$; $B = 1.5$; $\kappa^*/\epsilon^* = 1$; $\ell = 6$; $L = 24$

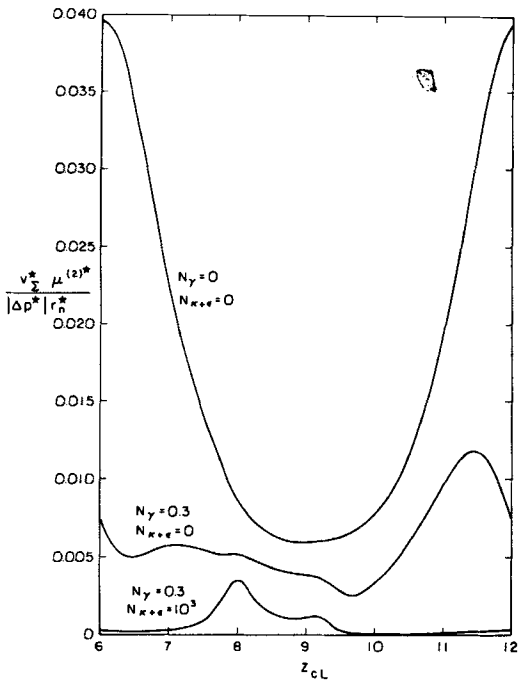

Figure 5. Axial speed of displacement for left interface of a segment of phase 2 being displaced through a pore initially filled with phase 1 as a function of axial position of left interface, Figure 3.

Values as in Figure 4.

For displacement in this system, $N_\gamma < 0.35$. The average flow rate through one pore unit ($6 < z < 12$) is shown in Figure 4. We see that, for $N_{\kappa+\epsilon} \gg 1$ and $N_\gamma < 0.35$, the percentage increase in $N_{\kappa+\epsilon}$ equals the percentage decrease in the flow rate for a fixed value of N_γ. We also find that the maximum variation in N_γ for a fixed value of $N_{\kappa+\epsilon}$ results in much smaller changes in the flow rate than do variations in $N_{\kappa+\epsilon}$ for a fixed value of N_γ. This means that when the interfacial tension is below that required for displacement ($N_\gamma < 0.35$), it is more important to reduce the interfacial viscosities than the interfacial tension.

This reinforces the conclusions of Slattery (1974, 1979) and of Giordano and Slattery (1983a) that an optimum surfactant formulation is one for which the interfacial tension is less than the critical value required for displacement and for which the interfacial viscosities are as small as possible. But caution is advised, since it remains to be demonstrated experimentally that there is a correlation between recovery efficiency and the interfacial viscosities.

Figure 5 shows the axial speed of displacement of the advancing (left) interface for the system described above. When interfacial effects are negligible, the interface accelerates as it approaches the pore neck and decelerates as it approaches the widest section of the pore. This motion is a result of conservation of mass and it should not be identified with a Haines (1930) jump, which we believe is the consequence of the limits of static stability in an irregular pore (Giordano and Slattery, 1983b). As interfacial effects become large, the displacement speed decreases and it becomes asymmetric with respect to the center of a pore unit ($z_{cL} = 9$).

Figure 6 indicates the variation of the volume rate of flow with position for the same system described by Figure 5. When interfacial effects are absent ($N_\gamma = N_{\kappa+\epsilon} = 0$), the volume rate of flow is relatively independent of the position of the segment of phase 2 in the capillary. The relatively small fluctuations in the flow rate occur because the distance between the left and right

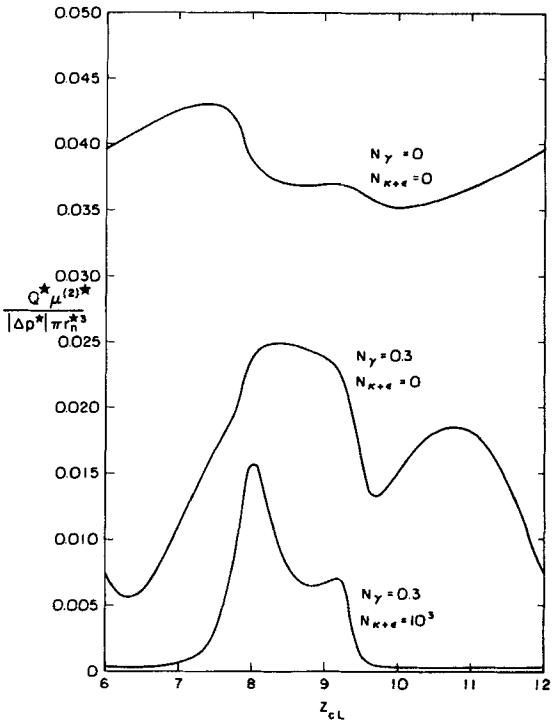

Figure 6. Flow rate through a capillary in which a segment of phase 2 is being displaced through a pore initially filled with phase 1 as a function of axial position of left interface, Figure 3.

Values as in Figure 4.

interfaces varies as the segment moves through the capillary, causing $z_{cL} - z_{cR}$ to change in Eq. 34.

When the effects of interfacial tension are taken into account but those of the interfacial viscosities are neglected ($N_\gamma = 0.3$, $N_{\kappa+\epsilon} = 0$), we see in Figure 6 that the flow is dominated by the effects of interfacial tension. Maxima and minima in the volume rate of flow occur as the interfaces successively accelerate and retard flow through the capillary. The locations of these maxima and minima depend upon the contact angles and the distance between the interfaces (the size of the segment). Comparison of our Figure 6 with Figure 6 (top curve) of Giordano and Slattery (1983b) (see also Figure 3 of Oh and Slattery, 1979) shows that for $N_{\kappa+\epsilon} = 0$ our periods of accelerating flow correspond to their regions of unstable, static states, and our periods of decelerating flow correspond to their regions of neutral stability. (In a state of neutral, static stability, a perturbation will not lead to spontaneous motion. But, because of contact-angle hysteresis, the interface may assume a new stable, static state that neighbors but is not identical to the original static state.)

The positions of these surges in the volume rate of flow change for large values of $N_{\kappa+\epsilon}$. Figure 6 shows that the effect of the interfacial viscosities ($N_\gamma = 0.3$, $N_{\kappa+\epsilon} = 10^3$) is to decrease the volume rate of flow relative to the case $N_{\kappa+\epsilon} = 0$ for all positions of the segment in the capillary. The effect of $N_{\kappa+\epsilon}$ will be minimized when the viscous dissipation in the interfaces, Eq. 28, is small. Since the dissipation depends in a complicated manner on axial position through K_1 and K_2, Eqs. 16 and 18, the variations in volume rate of flow shown in Figure 6 for $7 < z_{cL} < 10$ reflect variations in the interfacial viscous dissipation with position of the segment in the capillary. This shift reflects the increasing role of interfacial forces over bulk forces.

Note that there is no symmetry about the pore throat ($z_{cL} = 9$) when interfacial effects are present. This asymmetry occurs for two reasons. First, since the curvature of an interface will be the same at equidistant positions to the right and left of the pore throat only when the contact angle is 90°, in general the force generated by the interface will not be symmetric about the throat. Second, when there are two interfaces, as in this problem, the effect of the second interface is to add to the asymmetry.

At the leading or trailing edge of a large oil bank moving through a reservoir, we are concerned with the displacement of one phase by another, Figure 1, rather than with the mobilization of a segment of residual oil. Let us consider the same pore geometry as above and identify phase 1 as oil, phase 2 as brine, $\alpha = 140°$, and $N_\mu = 10$. Figure 7 indicates that the behavior of this system is qualitatively the same as that in which a segment of oil is displaced. The effect of the interfacial viscosities in Figure 7 occurs at a larger value of $N_{\kappa+\epsilon}$ than in Figure 4 because there is a contribution to the rate of surface viscous dissipation from only one interface and because the volume of the oil phase is comparatively larger. This suggests that the displacement of a single large segment will be less affected by the interfacial viscosities than a set of smaller segments (having the same total volume as the larger segment), since fewer interfaces are present. We again conclude that for an efficient tertiary oil recovery flood, the interfacial viscosities should be as small as possible.

Brown et al. (1982) found that during the displacement of crude oil by water in capillaries, there was a rolling motion (Dussan V. and Davis, 1974; Dussan V., 1977) in the crude oil-brine interface similar to that described here. In these systems, the interfacial viscosities have the potential to impede the displacement of crude oil.

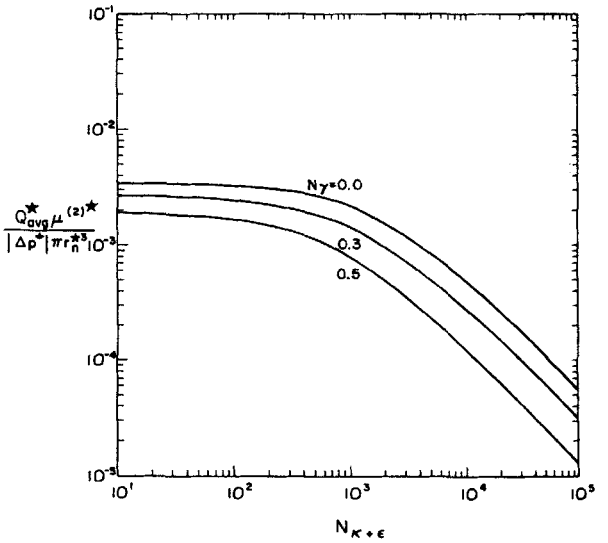

Figure 7. Average flow rate for displacement of phase 2 by phase 1 as a function of $N_{\kappa+\epsilon}$.
$N_\mu = 10$; $\alpha = 140°$; $B = 1.5$; $\ell = 6$; $L = 24$

In contrast, rigid interfacial films are found with other crude oil-brine systems (Reisberg and Doscher, 1956; Bourgoyne et al., 1972). Our analysis does not apply to such systems. A macroscopic interfacial film would be better modeled as a thin third phase separating the displacing and displaced phases.

Our analysis assumes that no wetting film exists between the capillary wall and the nonwetting phase. Legait (1983) has shown how a segment of oil is displaced through a capillary of variable square cross section when the displacing phase is continuous. Roof (1970; see also Arriola et al., 1980a,b) showed that, in completely water-wet capillaries, the water film forms a collar at the pore neck that can become unstable and "snap off" the oil into a series of droplets. Roof's criterion for snap-off requires

$$H_{ow} > H_n \tag{36}$$

where H_{ow} is the mean curvature of the oil-water interface and H_n is the mean curvature of the pore neck. For our sinusoidal capillary,

$$H_{ow} = -\left\{1 + \left[\frac{\pi B}{\ell}\sin\left(\frac{2\pi z_c}{\ell}\right)\right]^2\right\}^{-1/2} \cdot \left\{1 + \frac{B}{2}\left[1 - \cos\left(\frac{2\pi z_c}{\ell}\right)\right]\right\}^{-1} \tag{37}$$

and

$$H_n = \tfrac{1}{2}\,(2\pi^2 B/\ell^2 - 1) \tag{38}$$

In our analysis, we follow the recommendations of Oh and Slattery (1979) for sandstone rocks and set $B = 1.5$ and $\ell = 6$. For

this geometry, $H_{ow} \leq -0.43$ and $H_n = -0.089$. By Eq. 36, snap-off will not occur.

Additionally, Roof (1970) has shown that for systems displaying intermediate wettability as in our examples, oil-phase snap-off is unlikely. For oil segments that are long relative to their radius and separated from the capillary wall by a thin film of the continuous phase, instabilities can lead to breakup even in straight capillaries (Goren, 1962; Goldsmith and Mason, 1963). Our calculations assume that these types of instabilities are absent.

Although we have not considered the dynamics of the snap-off mechanism, it is reasonable to assume that snap-off will be retarded by the interfacial viscous forces resulting from the interfacial velocity gradients generated in the process.

Oh and Slattery (1979) recognized that for very large or small values of the contact angle, one phase will be trapped on the wall of a sinusoidal capillary during displacement. They used the term "discontinuous movement" to describe the apparent jump of the common line over this ring of trapped fluid. The analysis presented here does not allow for these discontinuous movements. Figure 8 describes the relationship between the onset of discontinuous motion, contact angle α, and ℓ. Here B_{min} is the minimum value of B required for discontinuous movements to occur. Incorporating discontinuous movements into our analysis would not be difficult, but it would give us little additional insight concerning the role of the interfacial viscosities during displacement.

Conclusions

The relative effects of the interfacial tension, the interfacial viscosities, and wetting on displacement in sinusoidal capillaries are quantitatively determined. The result is limited by assumptions that the Reynolds number N_{Re}, the capillary number N_{ca}, and the Bond number N_{Bo} are all small compared with unity and that surface viscous forces dominate bulk viscous forces in the interface (the dimensionless sum of the interfacial viscosities $N_{\kappa+\epsilon} \gg 1$).

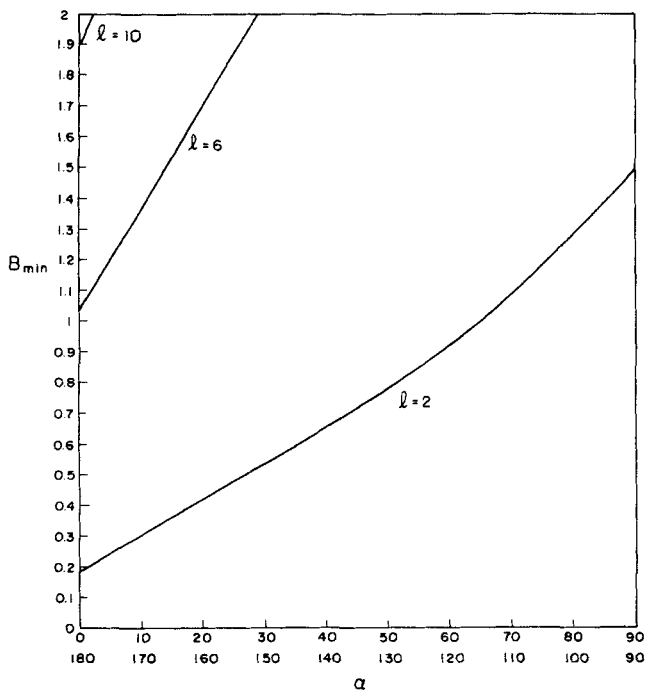

Figure 8. Minimum value of B required for discontinuous movements.

The limited data available for the interfacial viscosities of proposed tertiary oil recovery systems indicate that the dimensionless sum of the interfacial viscosities $N_{\kappa+\epsilon} \gg 1$.

For a displacement driven by a constant pressure drop, the effect of the interfacial viscosities is to decrease the rate of displacement regardless of the wetting condition. When $N_{\kappa+\epsilon} \gg 1$, a decrease in $N_{\kappa+\epsilon}$ causes an equal percentage increase in the volume rate of flow. This supports the conclusions our previous qualitative analysis (Slattery, 1974, 1979) and it is consistent with our previous analysis for displacement in straight, cylindrical capillaries (Giordano and Slattery, 1983a).

In screening surfactant systems for potential use in tertiary oil recovery, we recommend that the interfacial tension be minimized first, since it determines whether oil displacement will occur, and that the interfacial viscosities be minimized second, since they influence the rate of oil displacement.

Acknowledgment

The authors are grateful for financial support by the U.S. Department of Energy, Contract No. DE-AC19-79BC10068, Amoco Production Company, The Standard Oil Company (Ohio), and Union Oil Company of California.

Notation

A = defined by Eq. 9; see also Figure 2.
B = dimensionless value of B^*, Eq. 2
B^* = length characterizing capillary geometry, Figure 1
C = common line; constant, Eq. 22
C_0 = closed curve (circle) bounding Σ_0
$D^{(j)*}$ = rate of deformation tensor in phase j (Giordano and Slattery, 1983a)
$D^{(\sigma)*}$ = surface rate of deformation tensor (Giordano and Slattery, 1983a)
E = defined by Eq. 29
E_L, E_R = defined by Eq. 35
g = Acceleration of gravity
g_r = r-component of physical basis vector for cylindrical coordinate system in a frame of reference that is fixed with respect to a point on the common line
g_r, g_θ = physical basis vectors for spherical coordinate system in a frame of reference that is fixed with respect to center of curvature of the interface
g_z = unit vector parallel to axis of capillary
H = dimensionless mean curvature of interface, Eq. 3
H^* = mean curvature of interface; the sign depends upon the direction of ξ; the sign of $2H\,\xi$ is independent of the direction of ξ
H_n = dimensionless mean curvature of pore neck
H_{ow} = dimensionless mean curvature of oil-water interface
I = identity tensor
K_1, K_2 = Defined by Eqs. 16, 18
L^* = total length of $R_{(xyz)}$, Figure 1
ℓ = dimensionless length of a pore unit, Eq. 2
ℓ^* = length of a pore unit, Figure 1
n = unit normal directed outward with respect to $R_{(xyz)}$
N_{Bo} = bond number defined by $[\rho^{(1)*} - \rho^{(2)*}]g^* r_n^{*2}/\gamma^*$
N_{ca} = capillary number defined by $\mu^{(2)*} Q^*_{avg}/(\pi r_n^{*2}\gamma^*)$
$N^{(j)}_{Re}$ = Reynolds number for phase j, defined by $\rho^{(j)*} Q^*_{avg}/(\pi r_n^* \mu^{(j)*})$
N_γ = dimensionless interfacial tension, Eq. 31
$N_{\kappa+\epsilon}$ = dimensionless sum of interfacial viscosities, defined by $(\kappa^* + \epsilon^*)/(\mu^{(2)*} r_n^*)$
N_μ = viscosity ratio, Eq. 10

$p^{(j)}$ = dimensionless pressure in phase j, Eq. 3
$p^{(j)*}$ = pressure in phase j
Δp^* = pressure drop between $S^{(1)}$ and $S^{(2)}$, Figure 1
$|\Delta p^*|$ = magnitude of Δp^*
$\Delta p^{(j)}$ = pressure drop over one unit of a sinusoidal pore occupied by phase j, Eq. 22
P = projection tensor that transforms vectors defined on the dividing surface into their tangential components
P_ν^{-1}, $P_{\nu-1}^{-1}$ = associated Legendre functions of the first kind
Q^* = volume rate of flow
Q^*_{avg} = average volume rate of flow, Eq. 32
$\bar{r}$ = dimensionless spherical coordinate in a frame of reference fixed with respect to center of curvature of the interface, Eq. 3
$\bar{r}^*$ = spherical coordinate in a frame of reference fixed with respect to center of curvature of the interface
r_n^* = neck radius, Figure 1
r_w = dimensionless radius of capillary, Eq. 1
r_w^* = radius of capillary
r_{wc} = dimensionless radius of capillary at common line
r_{wc}^* = radius of capillary at common line
$R_{(yy)}$ = portions of phases 1 and 2 between $S^{(1)}$ and $S^{(2)}$, Figure 1
$S_{(yy)}$ = closed surface bounding $R_{(yy)}$
$S^{(1)}$, $S^{(2)}$ = imaginary entrance and exit surfaces, Figure 1
$S^{(j)}$ = dimensionless viscous portion of stress tensor in phase j, Eq. 3
$S^{(j)*}$ = viscous portion of stress tensor in phase j (Giordano and Slattery, 1983a)
$S^{(\sigma)}$ = dimensionless viscous portion of surface stress tensor, Eq. 3
$S^{(\sigma)*}$ = viscous portion of surface stress tensor (Giordano and Slattery, 1983a)
t = dimensionless time, Eq. 12
t^* = time
$T^{(j)*}$ = stress tensor in phase j
$T^{(\sigma)*}$ = surface stress tensor
$\bar{v}$ = dimensionless velocity viewed in a frame fixed with respect to center of curvature of the interface
$\hat{v}$ = dimensionless velocity viewed in a frame fixed with respect to a point on the common line
v = dimensionless velocity viewed in a frame fixed with respect to intersection of plane containing the common line and axis of the capillary, Figure 9
$v^{(j)}$ = dimensionless velocity in phase j, Eq. 3
$v^{(\sigma)}$ = dimensionless surface velocity, Eq. 3
$v^{(\sigma)*}$ = surface velocity
$\bar{v}^{(\sigma)}$ = dimensionless surface velocity viewed in a frame fixed with respect to center of curvature of the interface
$\bar{v}_\xi^\sigma$ = dimensionless theta component of surface velocity viewed in a frame fixed with respect to center of curvature of the interface
$\bar{v}_{(\sigma)}^{(\sigma)}$ = dimensionless normal component of surface velocity viewed in a frame fixed with respect to center of curvature of the interface
$\bar{v}_c$ = defined by Eq. 7
$\hat{v}_w$ = dimensionless velocity of capillary wall viewed in a frame fixed with respect to a point on the common line
v_Σ = dimensionless axial speed of displacement of interface viewed in a frame fixed with respect to capillary wall, Eq. 14
v_Σ^* = axial speed of displacement of interface viewed in a frame fixed with respect to the capillary wall
V_{drop} = defined as V^*_{drop}/r_n^{*3}
V^*_{drop} = volume of segment of phase 2, Figure 3
V^*_{pore} = volume of a unit pore
z = dimensionless axial position, Eq. 2
z^* = axial position, Figure 1
z_c = dimensionless axial position of common line viewed in a frame fixed with respect to wall
z_c^* = axial position of common line viewed in a frame fixed with respect to wall
$\bar{z}_c$ = dimensionless position vector of a point on common line viewed in a frame fixed with respect to center of curvature of the interface
$\hat{z}_0$, z_0 = dimensionless position vectors, Figure 9

Greek letters

α = contact angle measured through phase 1, Figure 1
α_{int} = intrinsic contact angle measured through phase 1
β = slope of capillary wall, Eq. 5
γ^* = interfacial tension
ϵ^* = interfacial shear viscosity
$\bar{\theta}$, $\bar{\phi}$ = spherical coordinates in a frame of reference fixed with respect to center of curvature of the interface
$\bar{\theta}_c$ = value of $\bar{\theta}$ at the common line
κ^* = interfacial dilatational viscosity
μ = unit vector that is normal to C and both tangent to and outwardly directed with respect to the interface
$\mu^{(j)*}$ = shear viscosity for phase j
ν = defined by Eq. 6
ξ = unit normal to phase interface
π = 3.1415...
$\rho^{(j)*}$ = total mass density of phase j
$\rho^{(\sigma)*}$ = total surface mass density
$\rho_0^{(\sigma)*}$ = total surface mass density in reference state
Σ = fluid-fluid interface, Figure 1
Σ_0 = portion of interface outside the immediate neighborhood of the common line
ϕ^* = potential energy per unit mass

Other terms

dA^* = an area integration is to be performed
ds^* = a line integration is to be performed
dV^* = a volume integration is to be performed
div = divergence operation
$\text{div}_{(\sigma)}$ = surface divergence operation (Wei et al., 1974; Briley et al., 1976)
tr = trace operation
∇ = gradient operator
$\nabla_{(\sigma)}$ = surface gradient operator (Wei et al., 1974; Briley et al., 1976)
L = subscript: left interface, Figure 3
R = subscript: right interface, Figure 3

Appendix A: Derivation of Eq. 11

Let $\bar{v}^{(\sigma)}$ denote the interfacial velocity defined in a frame of reference that is fixed with respect to the center of curvature of the interface; $\hat{v}^{(\sigma)}$ denotes the interfacial velocity defined in a frame of reference that is fixed with respect to the common line.

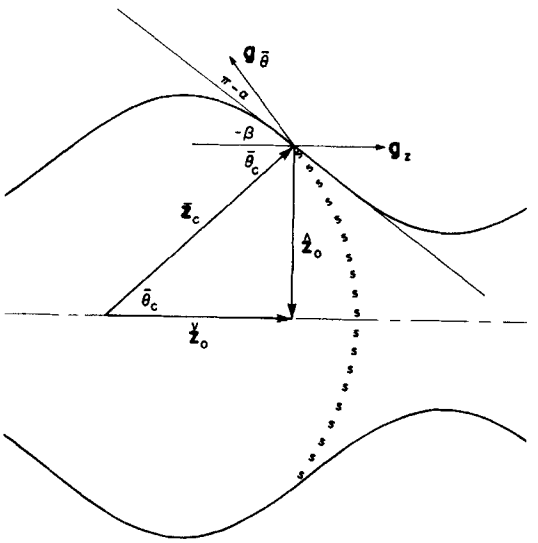

Figure 9a. Relationship of $\bar{z}_c$, $\hat{z}_0$, and z_0 for $\alpha + \beta > \pi/2$.

These surface velocities are related by

$$\bar{v}^{(\sigma)} = \hat{v}^{(\sigma)} + \frac{d\bar{z}_c}{dt} \tag{A1}$$

where $\bar{z}_c$ is the position vector of the common line in a frame of reference that is fixed with respect to the center of curvature of the interface.

Referring to Figure 9a, we see that when $\alpha + \beta > \pi/2$,

$$\bar{z}_c + \hat{z}_0 + z_0 = 0 \tag{A2}$$

$$\hat{z}_0 = -r_w g_r \tag{A3}$$

and

$$z_0 = -r_w \cot \bar{\theta}_c g_z \tag{A4}$$

which permits us to express Eq. A1 as

$$\bar{v}^{(\sigma)} \cdot g_{\bar{\theta}} = \hat{v}^{(\sigma)} \cdot g_{\bar{\theta}} + \frac{r_{wc}}{\sin \bar{\theta}_c} \frac{d\bar{\theta}_c}{dt} \tag{A5}$$

In arriving at Eq. A5, we have observed that

$$g_z \cdot g_{\bar{\theta}} = -\sin \bar{\theta}_c \tag{A6}$$

and

$$g_r \cdot g_{\bar{\theta}} = \cos \bar{\theta}_c \tag{A7}$$

Finally, since

$$\bar{\theta}_c = \alpha + \beta - \pi/2 \tag{A8}$$

we may rearrange Eq. A5 to obtain Eq. 11.

When $\alpha + \beta < \pi/2$ as in Figure 9b, we have in place of Eqs. A4 and A6

$$\bar{v}^{(\sigma)} \cdot g_{\bar{\theta}} = \hat{v}^{(\sigma)} \cdot g_{\bar{\theta}} + 2\frac{dr_{wc}}{dt} \cos \bar{\theta}_c - \frac{r_{wc}}{\sin \bar{\theta}_c} \frac{d\bar{\theta}_c}{dt} \tag{A9}$$

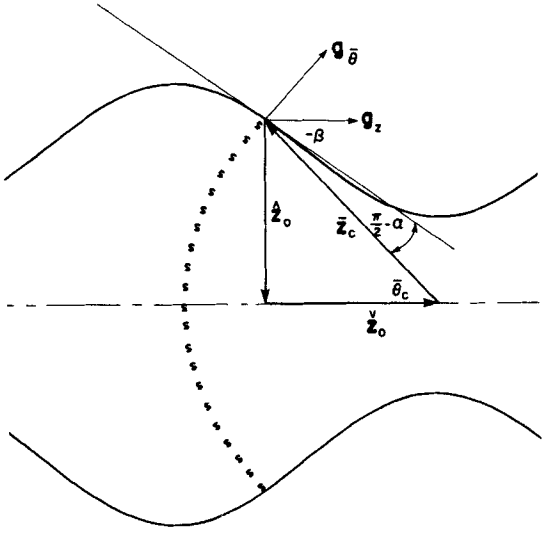

Figure 9b. Relationship of $\bar{z}_c$, $\hat{z}_0$, and z_0 for $\alpha + \beta < \pi/2$.

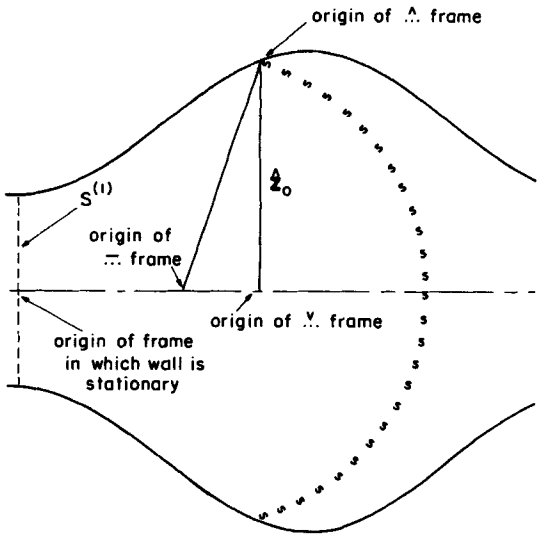

Figure 10. Relationship of a frame of reference that is fixed with respect to the intersection of the pore centerline and the plane containing the common line.

(Variables in this frame are denoted by ˇ...), a frame of reference that is fixed with respect to the center of curvature of the interface (variables in this frame are denoted by ¯...), and a frame of reference that is fixed with respect to a point on the common line (variables in this frame are denoted by ˆ...).

and

$$g_z \cdot g_{\bar{\theta}} = \sin \bar{\theta}_c \tag{A10}$$

Since

$$\bar{\theta}_c = \frac{\pi}{2} - \alpha - \beta \tag{A11}$$

Eq. A5 again reduces to Eq. 11.

Appendix B: Derivation of Eq. 15

Referring to Figure 10, let $\check{v}$ denote a velocity defined in a frame of reference that is fixed with respect to the intersection of the plane containing the common line and the axis of the capillary; let $\bar{v}$ be the same velocity observed in a frame of reference fixed with respect to the center of curvature of the interface; let v be the corresponding velocity measured in a frame of reference in which the capillary wall is stationary. These velocities are related by

$$v = \frac{dz}{dt} g_z + \check{v} \tag{B1}$$

and

$$\check{v} = \frac{dr_w}{dt} g_r + \hat{v} \tag{B2}$$

Since the velocity of the wall

$$v_w = 0 \tag{B3}$$

we see from Eqs. B1 and B2 that

$$\hat{v}_w = -\frac{dr_w}{dt} g_r - \frac{dz}{dt} \tag{B4}$$

In particular,

$$\text{at common line: } \hat{v}_w = -\frac{\pi B}{\ell} \sin\left(\frac{2\pi z_c}{\ell}\right) v_\Sigma g_r - v_\Sigma g_z \tag{B5}$$

Equation 15 gives the magnitude of this vector.

Literature Cited

Aleman, M. A., T. R. Ramamohan, and J. C. Slattery, "A Statistical Structural Model for Unsteady-State Displacement in Porous Media," SPE 13265, Soc. Pet. Eng. AIME, Richardson, TX (1984).

Arriola, A., G. P. Willhite, and D. W. Green, "Trapping of Oil Drops in a Noncircular Pore Throat," SPE 9404, Soc. Pet. Eng. AIME, Richardson, TX (1980a).

———, "Mobilization of an Oil Drop Trapped in a Noncircular Pore Throat upon Contact with Surfactants," SPE 9405, Soc. Pet. Eng. AIME, Richardson, TX (1980b).

Batra, V. K., and F. A. L. Dullien, "Correlation between Pore Structure of Sandstones and Tertiary Oil Recovery," *Soc. Pet. Eng. J.*, **13**, 256 (1973).

Bourgoyne, A. T., B. M. Caudle, and O. K. Kimbler, "The Effect of Interfacial Films in the Displacement of Oil by Water in Porous Media," *Soc. Pet. Eng. J.*, **12**, 60 (1972).

Briley, P. B., A. R. Deemer, and J. C. Slattery, "Blunt Knife-Edge and Disk Surface Viscometers," *J. Colloid Interf. Sci.*, **56**, 1 (1976).

Brown, C. E., T. J. Jones, and E. L. Neustadter, "The Measurement of Interfacial Forces during Crude Oil/Water Immiscible Displacement," *J. Can. Pet. Technol.*, **42** (May–June, 1982).

Dias, M. M., and A. C. Payatakes, "Network Models for Two-Phase Flow in Porous Media. 1: Immiscible Microdisplacement of Non-Wetting Fluids," *J. Fluid Mech.*, **164**, 305 (1986a).

———, "Network Models for Two-Phase Flow in Porous Media. 2: Motion of Oil Ganglia," *J. Fluid Mech.*, **164**, 337 (1986b).

Dussan V., E. B., "Immiscible Liquid Displacement in a Capillary Tube: the Moving Contact Line," *AIChE J.*, **23**, 131 (Jan., 1977).

Dussan V., E. B., and S. H. Davis, "On the Motion of a Fluid-Fluid Interface along a Solid Surface," *J. Fluid Mech.*, **65**, 71 (1974).

Geffen, T. M., "Oil Production to Expect from Known Technology," *Oil Gas J.*, 66 (May 7, 1973).

Giordano, R. M., and J. C. Slattery, "Effect of Interfacial Viscosities upon Displacement in Capillaries with Special Application to Tertiary Oil Recovery," *AIChE J.*, **29**, 483 (1983a).

———, "Stability of Static Interfaces in a Sinusoidal Capillary," *J. Colloid Interf. Sci.*, **92**, 13 (1983b).

Goldsmith, H. L., and S. G. Mason, "The Flow of Suspensions through Tubes. II: Single Large Bubbles," *J. Colloid Sci.*, **18**, 237 (1963).

Goren, S. L., "The Instability of an Annular Thread of Fluid," *J. Fluid Mech.*, **12**, 309 (1962).

Haines, W. B., "Studies in the Physical Properties of Soils. V: The Hysteresis Effect in Capillary Properties and the Modes of Moisture Distribution Associated Therewith," *J. Agric. Sci.*, **20**, 97 (1930).

Heller, J. P., "The Drying through the Top Surface of a Vertical Porous Column," *Proc. Soil Sci. Soc. Am.*, **32**, 778 (1968).

Jones, T. J., E. L. Neustadter and K. P. Whittingham, "Water-in-Crude Oil Emulsion Stability and Emulsion Destabilization by Chemical Demulsifiers," *J. Can. Pet. Technol.*, **17**(2), 100 (Apr.–June, 1978).

Legait, B., "Laminar Flow of Two Phases through a Capillary Tube with Variable Square Cross Section," *J. Colloid Interf. Sci.*, **96**, 28 (1983).

Legait, B., P. Sourieau, and M. Combarnous, "Inertia, Viscosity, and Capillary Forces During Two-Phase Flow in a Constricted Capillary Tube," *J. Colloid Interf. Sci.*, **91**, 400 (1983).

Lin, C. Y., and J. C. Slattery, "Three-Dimensional, Randomized, Network Model for Two-Phase Flow through Porous Media," *AIChE J.*, **28**, 311 (1982).

McConnell, A. J., *Applications of Tensor Analysis*, Dover, New York, 188 (1957).

Mohanty, K. K., H. T. Davis, and L. E. Scriven, "Physics of Oil Entrapment in Water-Wet Rock," SPE 13265, Soc. Pet. Eng. AIME, Richardson, TX (1980).

Morrow, N. R., "The Effects of Surface Roughness on Contact Angles with Special Reference to Petroleum Recovery," *J. Can. Pet. Technol.*, No. 4, 42 (Oct.–Dec., 1975).

Neira, M. A., and A. C. Payatakes, "Collocation Solution of Creeping Flow through Sinusoidal Tubes," *AIChE J.*, **25**, 725 (1979).

Oh, S. G., and J. C. Slattery, "Interfacial Tension Required for Significant Displacement of Residual Oil," *Soc. Pet. Eng. J.*, **19**, 83 (1979).

Reisberg, J., and T. M. Doscher, "Interfacial Phenomena in Crude Oil-Water Systems," *Prod. Mon.*, 43 (Nov., 1956).

Roof, J. G., "Snap-Off of Oil Droplets in Water-Wet Pores," *Soc. Pet. Eng. J.*, **10**, 85 (1970).

Rose, W., and R. W. Heins, "Moving Interfaces and Contact Angle Rate Dependency," *J. Colloid Sci.*, **17**, 39 (1962).

Slattery, J. C. "Interfacial Effects in the Entrapment and Displacement of Residual Oil," *AIChE J.*, **20**, 1145 (1974).

———, "Interfacial Effects in the Displacement of Residual Oil by Foam," *AIChE J.*, **25**, 283 (1979).

———, *Momentum, Energy, and Mass Transfer in Continua*, McGraw-Hill, New York (1972); 2nd ed., Krieger, Malabar, FL (1981).

Stoodt, T. J., and J. C. Slattery, "Effect of the Interfacial Viscosities upon Displacement," *AIChE J.*, **30**, 564 (1984).

Strassner, J. C., "Effect of pH on Interfacial Films and Stability of Crude Oil-Water Emulsions," *J. Petrol. Technol.*, 303 (Mar., 1968).

Teletzke, G., L. E. Scriven, and H. T. Davis, "Gradient Theory of Wetting Transitions," *J. Colloid Interf. Sci.*, **87**, 550 (1982).

Tilton, J. N., and A. C. Payatakes, "Collocation Solution of Creeping Newtonian Flow through Sinusoidal Tubes: A Correction," *AIChE J.*, **30**, 1016 (1984).

Wasan, D. T., S. M. Shah, N. Adegrangi, M. S. Chan, and J. J. McNamara, "Observations on the Coalescence Behavior of Oil Droplets and Emulsion Stability in Enhanced Oil Recovery," *Soc. Pet. Eng. J.*, **18**, 409 (1978).

Washburn, E. W., "The Dynamics of Capillary Flow," *Phys. Rev.*, **17**, 273 (1921).

Wayner, P. C. Jr., "Interfacial Profile in the Contact Line Region of a Finite Contact Angle System," *J. Colloid Interf. Sci.*, **77**, 495 (1980).

Wei, L. Y., W. Schmidt, and J. C. Slattery, "Measurement of the Surface Dilatational Viscosity," *J. Colloid Interf. Sci.*, **48**, 1 (1974).

Manuscript received Oct. 3, 1985, and revision received Apr. 6, 1987.